

# Supporting Information

## $\alpha,\beta$ -D-CNA induced rigidity within oligonucleotide

Christelle Dupouy<sup>a</sup>, Nathalie Iché-Tarrat<sup>a,b</sup>, Marie-Pierre Durrieu<sup>a</sup>, Alain Vigroux<sup>a</sup>, and Jean-Marc Escudier<sup>a,\*</sup>

<sup>a</sup> Laboratoire de Synthèse et Physico-Chimie de Molécules d'Intérêt Biologique, UMR 5068 CNRS, Université Paul Sabatier, 118 Route de Narbonne, 31062 Toulouse Cedex 9 (France)

<sup>b</sup> Centre d'Elaboration des Matériaux et d'Etudes Structurales, UPR 8011 CNRS, 29 rue Jeanne Marvig, 31055 Toulouse Cedex 4 (France)

[\*] fax: (+33)5-6155-6011

E-mail: [escudier@chimie.ups-tlse.fr](mailto:escudier@chimie.ups-tlse.fr)

## CONTENTS

Oligonucleotide synthesis and characterization	S2
Thermal denaturation experiments	S2-S4
Circular dichroism experiments	S5-S10

## Oligonucleotides synthesis

The oligonucleotides were assembled on CPG support (1  $\mu$ mol scale) on a ABI 394 using the standard phosphoramidite chemistry. After complete assembly of the oligonucleotide chain, deprotection were achieved with  $\text{NH}_4\text{OH}$  (33%) at 25  $^\circ\text{C}$  for 24 h. The crude product was analysed and purified by reversed phase HPLC (Kromasil  $\text{C}_{18}$ , 7  $\mu\text{m}$ , 100  $\text{\AA}$ , 250 x 4.6 mm for analysis or 250 x 20 mm for purification scale) on a Waters apparatus (600 E pump system controller and a 996 photodiode array detector), using a gradient from 95% of A to 70% of A in B (A: TEAA buffer 0.05 M, pH 7.0; B:  $\text{CH}_3\text{CN}$ ). Analysis of the oligonucleotides were performed by mass spectrometry in MALDI TOF mode on a PerSeptive Biosystems Voyager Spectrometer with THAP, 10% ammonium citrate as matrix.

**Table S1** : MALDI-TOF-MS, HPLC Purification ( $t_{\text{R}}$ ), and Yield of oligonucleotides containing **TT** = ( $R_{\text{C5}}$ ,  $S_{\text{P}}$ )  $\alpha,\beta$ -D-CNA TT.

ODN	Sequence	MW calculated	MW found	$t_{\text{R}}$ min	OD (260nm) (yield[%])
<b>2</b>	5'-TTTT <b>TT</b> TTTT	3006.0	3006.1	17.1	52.2 (64)
<b>4</b>	5'-TTTTTT <b>TT</b> TTTTTT	4222.8	4221.8	17.4	49.0 (43)
<b>6</b>	5'-GCAAAAAG <b>TT</b> GTC	3664.4	3663.8	14.9	26.8 (22)
<b>7</b>	5'-GCAACT <b>TT</b> TTTGC	3674.5	3673.9	15.9	28.5 (27)
<b>8</b>	5'-GCAACT <b>TT</b> TTTGC	3674.5	3675.1	15.9	30.7 (29)
<b>9</b>	5'-GCAACT <b>TT</b> TTGTC	3674.5	3673.5	15.4	22.2 (21)
<b>10</b>	5'-GCAACTTT <b>TT</b> GTC	3674.5	3674.7	15.2	32.8 (31)

## Thermal denaturation studies

Absorbance versus temperature profiles were recorded at 260 nm in fused quartz cuvettes on a Carry 300 Bio spectrophotometer equipped with a Peltier temperature control device. Each sample are heated to 90  $^\circ\text{C}$  and then slowly cooled before measurements. The temperature is increased by 0.5  $^\circ\text{C}/\text{min}$  from 3 or 10 to 90  $^\circ\text{C}$ . The two complementary strands were in 5 to 10  $\mu\text{M}$  range concentration (10mM phosphate buffer, pH 7.00, 100 mM NaCl, 1 mM EDTA) assuming identical extinction coefficient for the  $\alpha,\beta$ -D-CNA including oligonucleotide and

the corresponding unmodified ones. Melting temperatures were calculated by use of the Carry software.

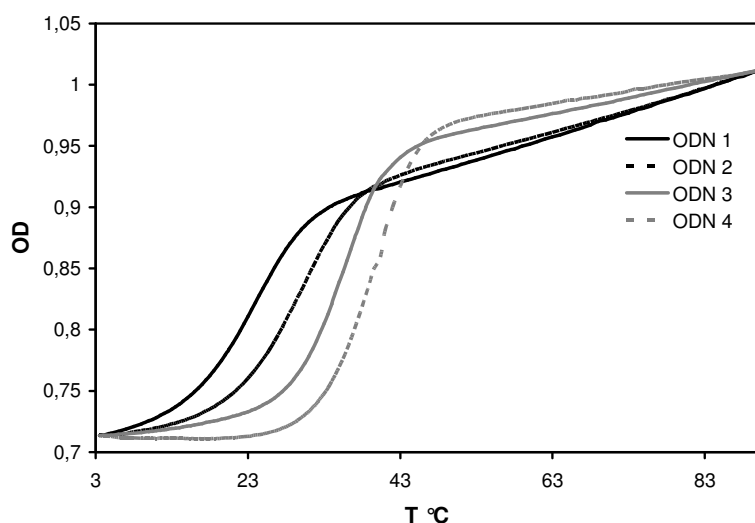


**Figure S1.** Thermal denaturation curves (table 1, entries 1-4), for 5'-dA<sub>14</sub> with unmodified 5'-dT<sub>10</sub> (ODN 1) or dT<sub>14</sub> (ODN 3), or with 5'-dT<sub>4</sub>TTT<sub>4</sub> (ODN 2) or 5'-dT<sub>6</sub>TTT<sub>6</sub> (ODN 4), TT = (R<sub>C5'</sub>, S<sub>P</sub>) α,β-D-CNA TT.

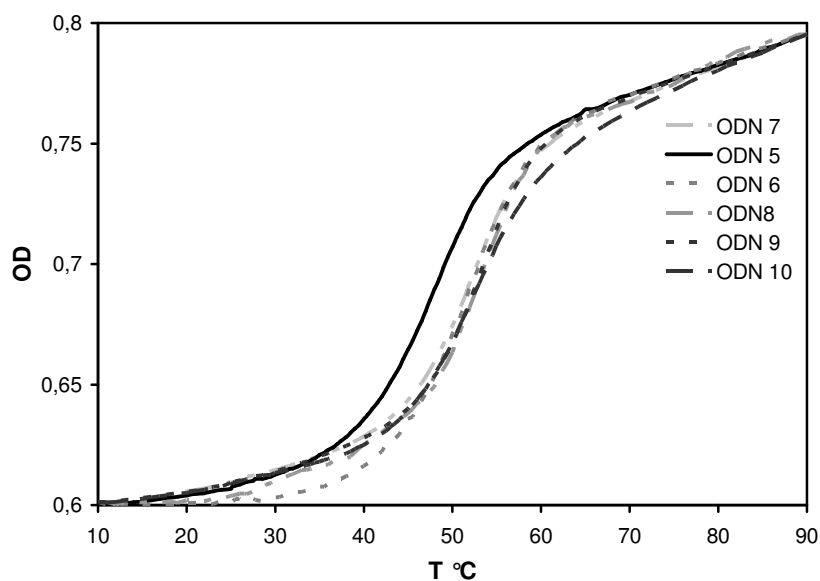


**Figure S2.** Thermal denaturation curves (table 1, entries 5, 7-10), for 5'-d(GCAAAAACCTTGC) with unmodified 5'-d(GCAAGTTTTTGC) (ODN 5), or with 5'-d(GCAAGTTTTTTGC) (ODN 7) or 5'-d(GCAAGTTTTTTTGC) (ODN 8) or 5'-d(GCAAGTTTTTTTTGC) (ODN 9) or 5'-d(GCAAGTTTTTTTTGC) (ODN 10) and thermal denaturation curve (table 1, entry 6), for 5'-d(GCAAAAACTTGC) with unmodified 5'-d(GCAAGTTTTTGC). TT = (R<sub>C5'</sub>, S<sub>P</sub>) α,β-D-CNA TT.

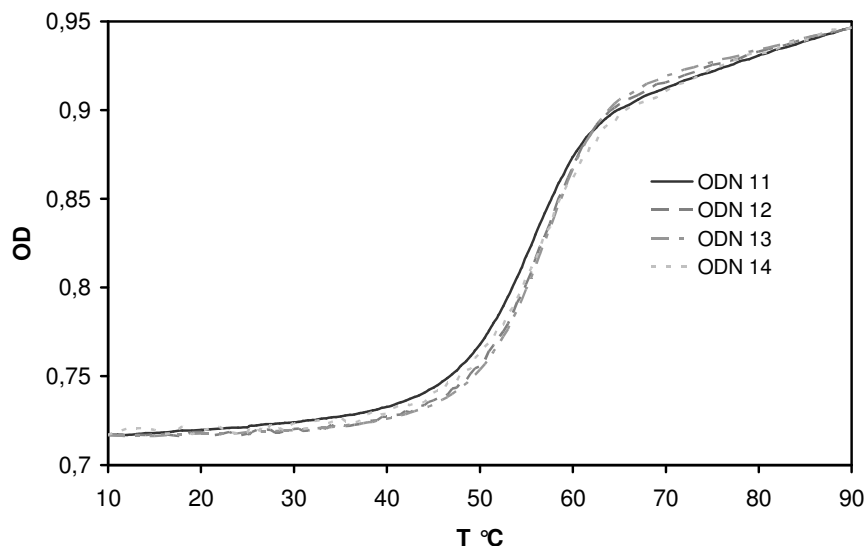


**Figure S3.** Thermal denaturation curves (table 1, entries 11-14) for 5'-d(GCAAAACTTGC) with 5'-d(GCAAGTTTTGC) (**ODN 11**) or 5'-d(GCAAGTTTTGC) (**ODN 12**) or 5'-d(GCAAGTTTTGC) (**ODN 13**) or 5'-d(GCAAGTTTTGC) (**ODN 14**), TT = ( $R_{CS}$ ,  $S_P$ )  $\alpha,\beta$ -D-CNA TT.

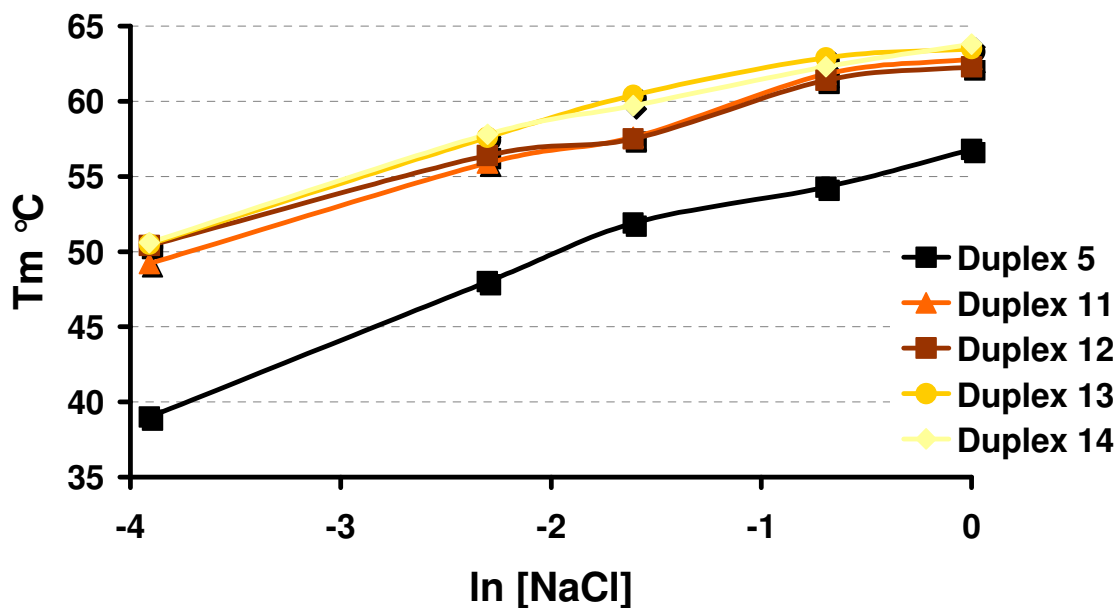


**Figure S4.**  $T_m$  vs.  $\ln[\text{NaCl}]$  plots of the five duplexes indicated ( $c = 5\mu\text{M}$ , 10mM phosphate buffer, pH 7.00, 100 mM NaCl, 1 mM EDTA)

### Circular dichroism studies.

These experiments were carried out on a Jasco J-815 CD spectrometer equipped with a Peltier controller Jasco PTC-4235/15 at a duplex concentration range of 5  $\mu\text{M}$  in a 10 mM  $\text{Na}_2\text{HPO}_4$ , 100 mM NaCl, 0.1 mM  $\text{Na}_2\text{EDTA}$ , buffer, pH  $7.00 \pm 0.02$ . Molar extinction coefficients were calculated from those of dinucleotides using the nearest-neighbor approximation method assuming that  $\alpha,\beta\text{-D-CNA TT}$  have the same molar extinction coefficient as TpT. Dinucleotide concentration was determined from UV absorbance at high temperature (90  $^\circ\text{C}$ ). All CD spectra were recorded after stabilization of the temperature for 10 min and were normalized by subtraction of the background scan with buffer. Taking the known dinucleotide concentration into account, the normalized spectra were converted to variation of molar extinction coefficient ( $\Delta\epsilon$ ).

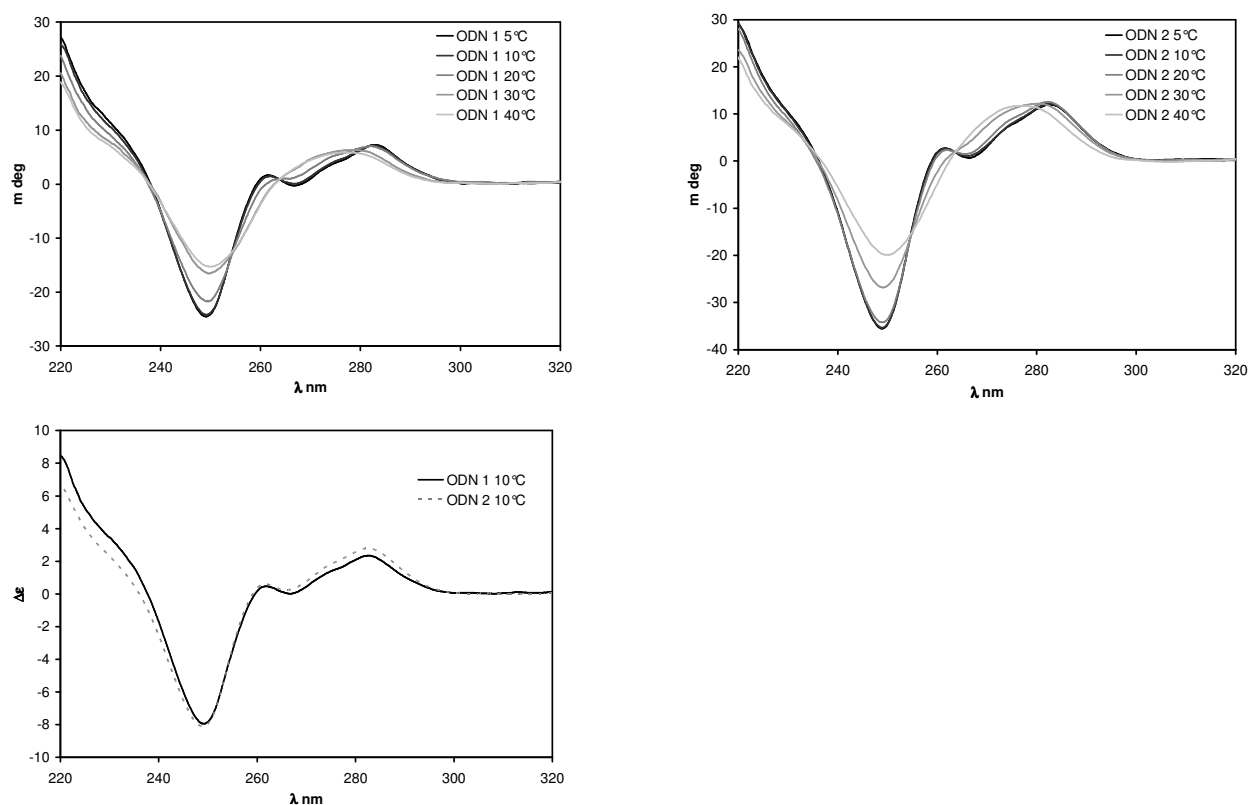


**Figure S5.** CD spectra as a function of temperature of the duplexes (table 1, entries 1, 2), for 5'-dA<sub>14</sub> with unmodified 5'-dT<sub>10</sub> (ODN 1), or with 5'-dT<sub>4</sub>TTT<sub>4</sub> (ODN 2), TT = ( $R_{C5'}$ ,  $S_P$ )  $\alpha,\beta\text{-D-CNA TT}$ .

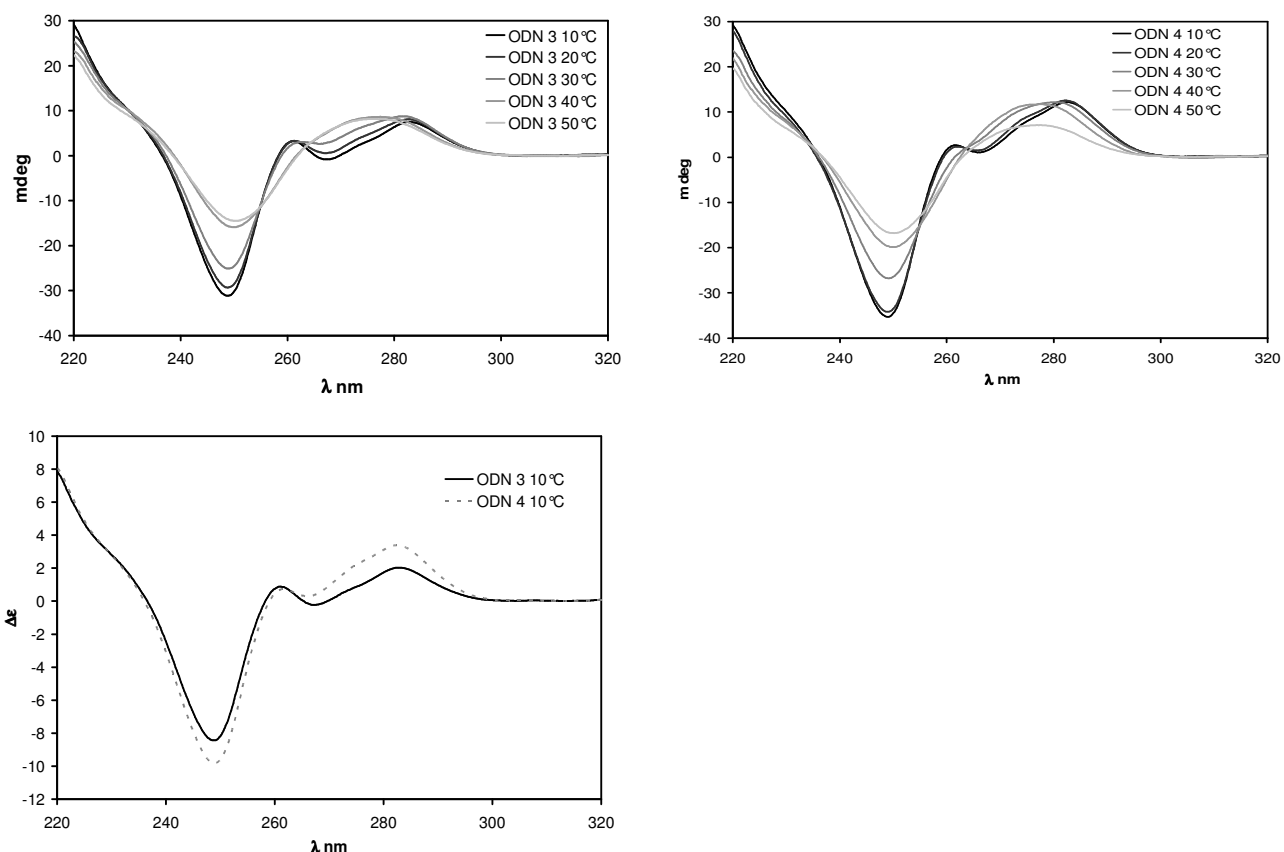


**Figure S6.** CD spectra as a function of temperature of the duplexes (table 1, entries 3, 4), for 5'-dA<sub>14</sub> with unmodified 5'-dT<sub>14</sub> (**ODN 3**), or with 5'-dT<sub>6</sub>TTT<sub>6</sub> (**ODN 4**), TT = (*R*<sub>C5'</sub>, *S*<sub>P</sub>) α,β-D-CNA TT.

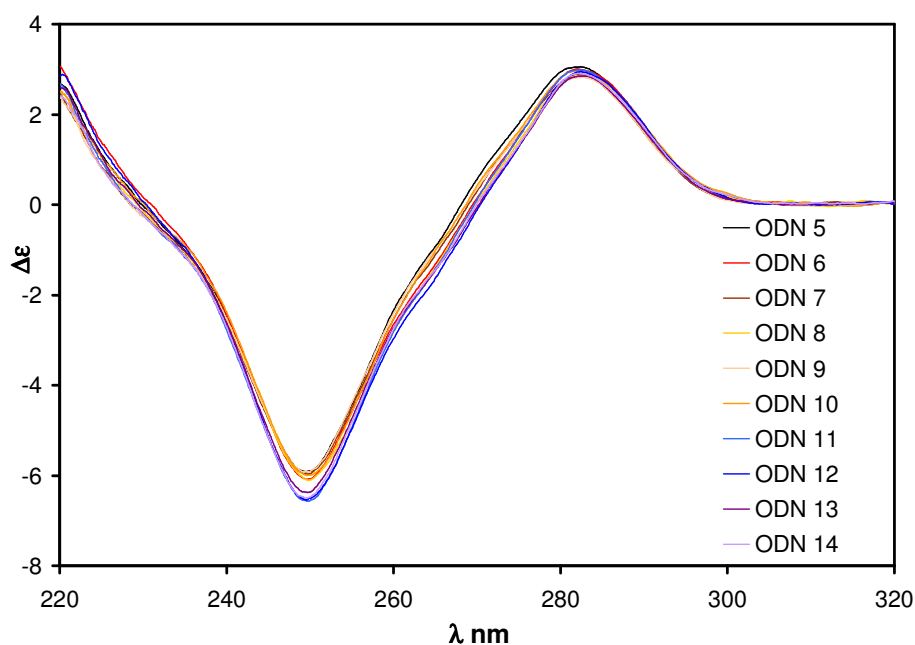


**Figure S7.** CD spectra of the duplexes (table 1, entries 5 to 14) 5'-d(GCAAAAACCTTGC)/5'-d(GCAAGTTTTTGC) (unmodified, **ODN 5**), including one α,β-D-CNA TT (**ODN 6-10**) or two α,β-D-CNA TT (**ODN 11-14**), in sodium phosphate (10 mM, pH 7.0), NaCl (100 mM) and EDTA (1mM), T = 20°C. Duplex concentration ~ 5 μM.

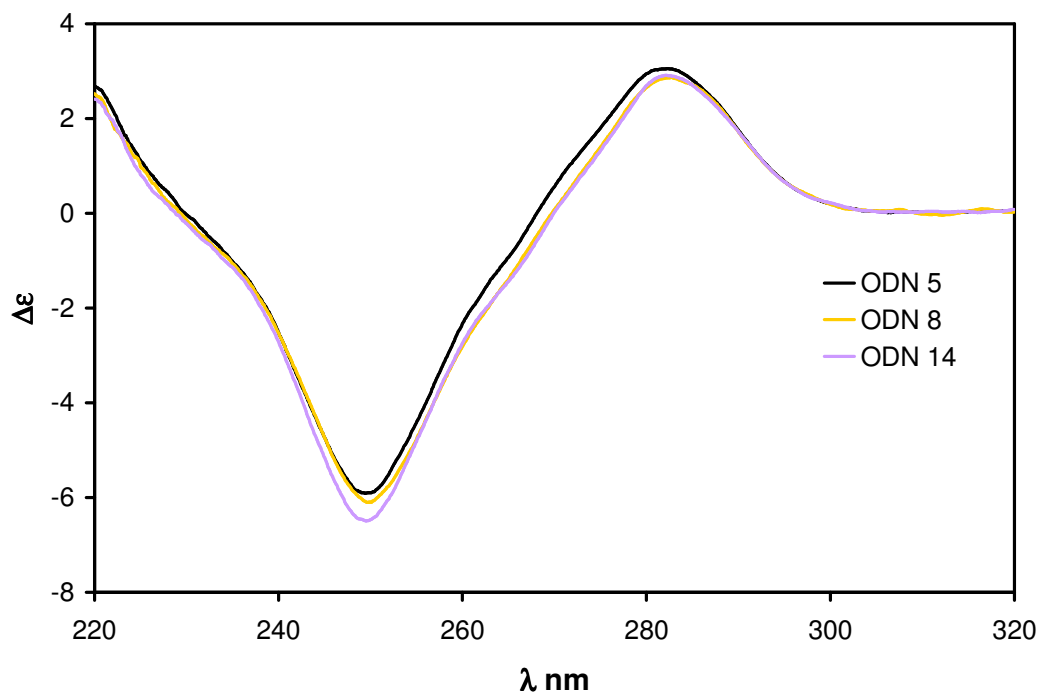


**Figure S8.** CD spectra of unmodified 5'-d(GCAAAAACCTTGC)/5'-d(GCAAGTTTTTGC) (**ODN 5**), compared with those of **ODN 8** incorporating one  $\alpha,\beta$ -D-CNA TT and with **ODN 14** incorporating two  $\alpha,\beta$ -D-CNA TT within duplex (table 1, entries 5, 8 and 14) in sodium phosphate (10 mM, pH 7.0), NaCl (100 mM) and EDTA (1mM), T = 20°C. Duplex concentration ~ 5  $\mu$ M.

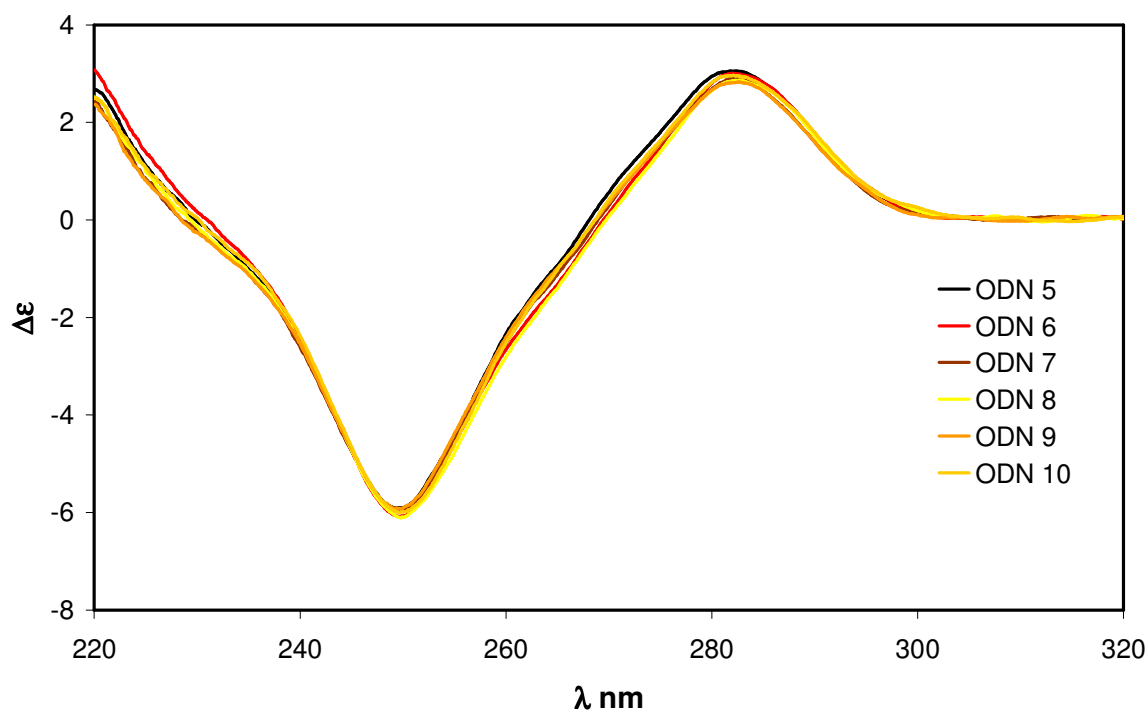


**Figure S9.** CD spectra of unmodified 5'-d(GCAAAAACCTTGC)/5'-d(GCAAGTTTTTGC) (**ODN 5**), compared with those of **ODN 6-10** incorporating one  $\alpha,\beta$ -D-CNA TT (table 1, entries 5 and 11-14) in sodium phosphate (10 mM, pH 7.0), NaCl (100 mM) and EDTA (1mM), T = 20°C. Duplex concentration ~ 5  $\mu$ M.

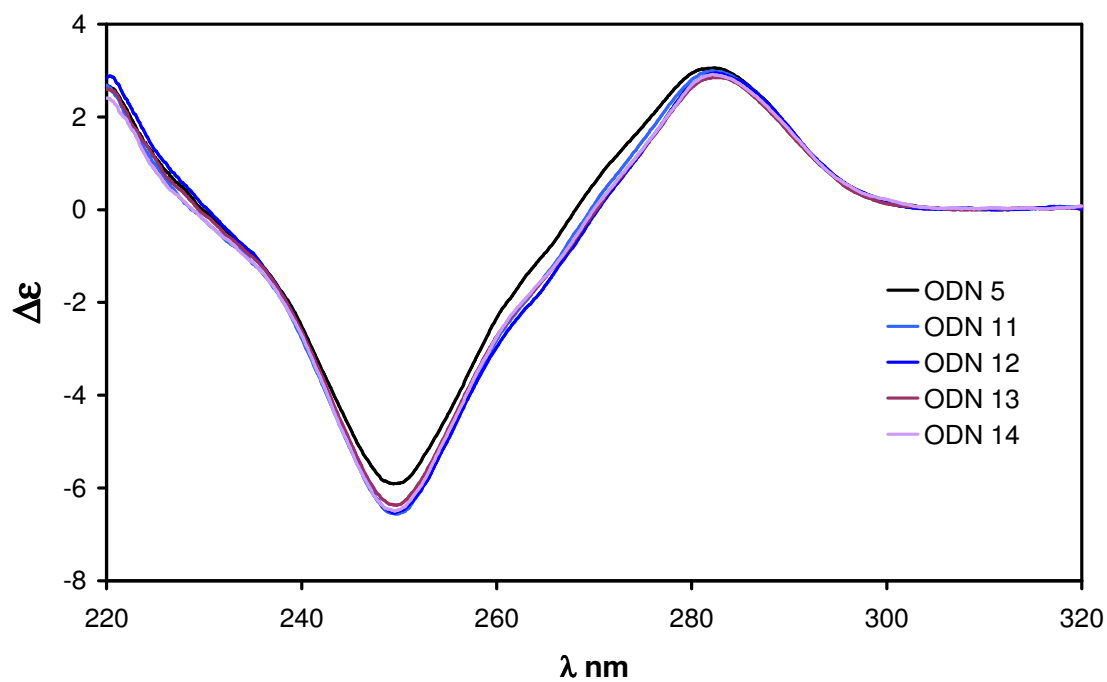


**Figure S10.** CD spectra of unmodified 5'-d(GCAAAAACCTTGC)/5'-d(GCAAGTTTTTGC) (**ODN 5**), compared with those of **ODN 11** to **14** incorporating one  $\alpha,\beta$ -D-CNA TT on each strand within duplex (table 1, entries 5 and 11-14) in sodium phosphate (10 mM, pH 7.0), NaCl (100 mM) and EDTA (1mM), T = 20°C. Duplex concentration ~ 5  $\mu$ M.